Neurochemistry International 194 (2026) 106134

Contents lists available at ScienceDirect

Neurochemistry International

journal homepage: www.elsevier.com/locate/neuint

Retinoic acid signaling regulates astrocyte reactivity by modulating MAPK/NF-κB pathways and mitochondrial integrity

Seo Hyun Yoo [a,1], Dongyun Kim [a,1], Gyu-Bum Yeon [a,b,1], Jaeyeon Choi [a], Jaewook Lee [a], Dong-Wook Kim [c], Hyunggee Kim [a,b,*], Dae-Sung Kim [a,b,d,**]

[a] Department of Biotechnology, College of Life Sciences and Biotechnology, Korea University, Seoul, Republic of Korea
[b] Institute of Animal Molecular Biotechnology, Korea University, Seoul, Republic of Korea
[c] Department of Physiology, Yonsei University College of Medicine, Seoul, Republic of Korea
[d] Department of Pediatrics, Korea University College of Medicine, Guro Hospital, Seoul, Republic of Korea

ARTICLE INFO

Keywords:
Astrocyte
Reactive astrocytes
Induced pluripotent stem cell (iPSC)
Neuroinflammation
Retinoic acid
Inflammatory cytokines

ABSTRACT

Astrocytes respond to inflammatory stimuli by adopting a reactive state characterized by morphological, molecular, and functional changes that affect tissue repair and disease progression. A key feature of this transformation is the metabolic shift that supports inflammatory signaling and cytokine production. Retinoic acid (RA) modulates immune responses in the peripheral system; however, its role in astrocyte reactivity remains poorly understood. In this study, we investigated alterations in RA metabolism using an *in vitro* model of reactive astrocytes derived from human pluripotent stem cells. Reactivity was induced by treatment with tumor necrosis factor-α (TNF-α), interleukin-1α (IL-1α), and complement component 1q (C1q), collectively referred to as TIC, and characterized using comprehensive morphological, molecular and functional analyses. We found that the induced reactive astrocytes exhibited a marked downregulation of key biosynthetic enzymes in RA metabolism, leading to a net decrease in intracellular RA levels. Exogenous RA supplementation attenuated TIC-induced expression of pro- and anti-inflammatory mediators, including IL-6, IL-8, nitric oxide, IL-10, and TGFβ. Mechanistically, RA suppressed these inflammatory responses by inhibiting NF-κB activation, likely through upstream attenuation of ERK and p38 MAPK pathways via upregulation of MAPK phosphatase 1 (MKP-1). In neuron and TIC-treated astrocyte co-cultures, RA treatment reduced the density of cleaved caspase 3-positive apoptotic-like neurons, an effect accompanied by decreased nitric oxide levels. These observations coincided with the restoration of mitochondrial integrity and mitophagy. Taken together, these findings identify RA metabolism as a key regulatory node in astrocyte reactivity and suggest a potential therapeutic role for RA in neuroinflammatory conditions.

1. Introduction

Astrocytes are the most abundant glial cells in the central nervous system (CNS), which play essential roles in maintaining neuronal homeostasis, supporting synaptic transmission, and regulating the blood-brain barrier (Alvarez et al., 2013; Chung et al., 2015; Khakh and Sofroniew, 2015). Additionally, these cells form intricate interactions with neurons throughout the brain and spinal cord, where they perform essential functions such as neurotransmitter clearance, ion buffering, and metabolic support for neurons (Belanger et al., 2011; Duan et al., 1999). Under physiological conditions, astrocytes exhibit a homeostatic phenotype defined by distinctive morphological and molecular characteristics that support CNS function. However, in response to pathological insults such as infection, trauma, or neurodegeneration, astrocytes undergo a transformation known as "astrocyte reactivity," characterized by significant changes in morphology, gene expression, and functional output (Sofroniew and Vinters, 2010). Rather than representing a simple binary shift, this process spans a continuum of cellular states, with astrocytes adopting diverse phenotypes depending on the cellular context, nature, and severity of the triggering stimulus (Escartin et al., 2021;

* Corresponding author. Department of Biotechnology, Korea University, 145 Anam-ro, Seongbuk-gu, Seoul 02841, Republic of Korea.
** Corresponding author. Department of Biotechnology, Korea University, 145 Anam-ro, Seongbuk-gu, Seoul 02841, Republic of Korea.
E-mail addresses: hg-kim@korea.ac.kr (H. Kim), sonnet10@korea.ac.kr (D.-S. Kim).
[1] These authors contributed equally to this work.

https://doi.org/10.1016/j.neuint.2026.106134
Received 23 December 2025; Received in revised form 6 February 2026; Accepted 19 February 2026
Available online 20 February 2026
0197-0186/© 2026 The Authors. Published by Elsevier Ltd. This is an open access article under the CC BY license (http://creativecommons.org/licenses/by/4.0/).

Zamanian et al., 2012; Zhang et al., 2025). Among the various phenotypes, the subtype induced by a combination of inflammatory mediators—tumor necrosis factor-α (TNF-α), interleukin-1α (IL-1α), and complement component 1q (C1q) (collectively referred to as TIC)—is particularly noteworthy due to its well-documented inflammatory and neurotoxic properties, and involvement in various neurological conditions, including Alzheimer's disease (AD), multiple sclerosis (MS), and amyotrophic lateral sclerosis (Liddelow et al., 2017). TIC-induced reactive astrocytes are characterized not only by an inflammatory transcriptional profile but also by substantial functional alterations. This reactive state is associated with a loss of key homeostatic functions, including glutamate recycling and phagocytic clearance of synaptic debris, while concurrently acquiring neurotoxic properties. Recent studies have demonstrated that the astrocytes secrete neurotoxic factors, such as long-chain saturated lipids, which contribute to neuronal and oligodendrocyte damage (Guttenplan et al., 2021; Liddelow et al., 2017). Crucially, these broad functional impairments are closely linked to sustained inflammatory cytokine production and intracellular metabolic dysregulation. Thus, elucidating the mechanisms that regulate this inflammatory phenotype is essential for restoring astrocyte homeostasis.

In recent years, astrocytes derived from human pluripotent stem cells (hPSCs), including human embryonic stem cells and human induced pluripotent stem cells (hiPSCs), have emerged as powerful tools for investigating astrocyte reactivity and its implications in CNS diseases (Barbar et al., 2020; Leng et al., 2022). Efficient differentiation protocols followed by exposure to inflammatory stimuli, such as TIC, have enabled detailed exploration of the molecular and cellular pathways underlying astrocyte activation (Leng et al., 2022). These hPSCs-based models provide unprecedented opportunities to determine the contribution of reactive astrocytes to CNS inflammation at mechanistic and translational levels. One of the most notable aspects of astrocytic reactivity is the extensive reprogramming of cellular metabolism, which is accompanied by functional transformation. Similar to immune cells, reactive astrocytes undergo a metabolic shift to meet the increased biosynthetic and energetic demands associated with inflammation (Chen et al., 2023; Pamies et al., 2021; Robb et al., 2020). Consequently, metabolic reprogramming is now recognized as a hallmark of glial activation in the CNS; however, the precise biochemical pathways involved and upstream regulatory mechanisms remain unclear. Elucidating these changes is critical, because metabolic pathways are promising therapeutic targets for modulating astrocyte function in neuroinflammatory disorders.

Retinoic acid (RA), with its all-*trans* form being the most biologically active among its isomers, is a multifunctional signaling molecule whose biological actions extend well beyond its classical role in vision (Napoli, 2012). RA biosynthesis is a tightly regulated, multistep enzymatic process (Gudas, 2022). The initial conversion of retinol to retinaldehyde is catalyzed by retinol dehydrogenases, such as retinol dehydrogenase 10 (RDH10) and dehydrogenase/reductase 9 (DHRS9). This step is modulated by reductases, such as DHRS3 and DHRS13 (Seo et al., 2025), which act in the reverse direction and help fine-tune retinaldehyde synthesis. The subsequent rate-limiting step, which converts retinaldehyde to RA, is mediated by the aldehyde dehydrogenase 1A family members (ALDH1A1, ALDH1A2, and ALDH1A3). ALDH1A enzymes are pivotal for RA synthesis because their expression levels directly dictate the cellular capacity for RA production, thereby serving as critical regulatory checkpoints for RA homeostasis. Meanwhile, RA catabolism is primarily carried out by cytochrome P450 26A1 (CYP26A1), which degrades RA and terminates its signaling pathway. Thus, the balance between RA synthesis and breakdown determines its bioavailability and functional impact on astrocytes. Once produced, RA modulates gene expression primarily through a genomic mechanism involving binding to the RA receptor (RAR) and retinoid X receptor (RXR) heterodimers, which interact with RA response elements (RAREs) in the promoters of target genes (di Masi et al., 2015). Previous studies have demonstrated that RA suppresses pro-inflammatory signaling cascades, including NF-κB, STAT1, and AP-1 pathways, leading to reduced expression of key cytokines such as TNF-α, IL-6, and IL-1β (Chen et al., 2002; Zhou et al., 1999). In addition to these transcriptional effects, RA exerts rapid non-genomic actions by modulating kinase signaling pathways, such as extracellular signal-regulated kinase 1/2 (ERK1/2) and p38 mitogen-activated protein kinase (MAPK) (Huang et al., 2008; Yen et al., 1998). Furthermore, within the CNS, RA has been implicated in various neurodevelopmental and neurodegenerative disorders (Maden, 2007). Emerging evidence suggests that RA may also attenuate neuroinflammatory responses by limiting the activation of astrocytes and microglia (Kampmann et al., 2008; Kim et al., 2008; van Neerven et al., 2010; Xu and Drew, 2006). However, the specific anti-inflammatory mechanisms of RA and the biological background of why RA is required to modulate the reactivity of astrocytes remain poorly understood and understudied in the context of CNS inflammation. The intersection of RA metabolism with astrocyte reactivity is a critical but underexplored area in neuroinflammatory research. Consequently, understanding this relationship is particularly important, considering the growing interest in targeting cellular metabolism as a therapeutic strategy for chronic neuroinflammatory conditions.

Given these considerations, our study aimed to: 1) develop and validate a hiPSC-based model of reactive astrocytes induced by the TIC cytokine cocktail; 2) characterize changes in RA metabolic pathways in these cells; 3) evaluate the effects of exogenous RA on astrocyte reactivity and inflammatory responses; and 4) elucidate the molecular mechanisms by which RA modulates key signaling pathways involved in inflammatory responses in reactive astrocytes. Through this integrative approach, we aimed to provide insight into the role of RA in astrocyte reactivity and establish its potential as a therapeutic target for neuroinflammatory diseases.

2. Experimental procedures

2.1. Culture and neural differentiation of hiPSCs

In this study, a hiPSC line (NL1) (Yeon et al., 2021) were maintained in StemMACS™ iPS-Brew XF culture medium (Miltenyi Biotec, North Rhine-Westphalia, Germany) using 6-well culture plates pre-coated with Matrigel (Corning, NY, USA). Cell expansion was achieved using enzymatic passaging methods using Accutase (Thermo Fisher Scientific, MA, USA) with the addition of Y27632 (10 μM) (Millipore Sigma, MO, USA) to enhance cell survival during passaging. The differentiation of hiPSCs to neural precursor cells (NPCs) was accomplished using a dual-SMAD inhibition approach, following established protocols with slight modifications (Chambers et al., 2009). The procedure involved enzymatic dissociation of hiPSCs into single cells, followed by seeding at a density of 3×10^4 cells/cm^2 onto Matrigel-coated culture vessels. The initial plating medium consisted of StemMACS™ iPS-Brew XF supplemented with 10 μM Y27632. Neural differentiation was initiated on the following day by transitioning cells to StemMACS™ iPS-Brew XF medium supplemented with 500 nM LDN193189 (Selleck Chemicals, TX, USA) and 10 μM SB431542 (Millipore Sigma). Cells were cultured in the differentiation medium for 8 days. Successful NPCs generation was confirmed when more than 80% of the cell population expressed SOX1 on days 8–10 of differentiation. The validated NPCs were either utilized for subsequent astrocyte differentiation protocols or preserved in liquid nitrogen for future experimental applications.

2.2. Production of lentivirus

Lentiviral vectors were produced by co-transfecting 293 FT cells with plasmids encoding rtTA (Addgene #20342, MA, USA), nuclear factor I B (NFIB), neurogenin 2 (Ngn2), or mito-SRAI (#RDB18223) along with packaging plasmids pMDLg/pRRE, pRSV-Rev, and envelope plasmid pMD2.G (Addgene #12251, #1225, and #12,259, respectively) using Lipofectamine® 3000 (Thermo Fisher Scientific, MA, USA) according to the manufacturer's instructions. Viral supernatants were collected 72 h

after transfection and concentrated using a Lenti-X concentrator (Takara, Kusatsu, Japan). After determining viral titers, concentrated lentiviral stocks were aliquoted and stored at −80 °C. Additional NFIB-overexpressing lentiviruses were obtained from an external service provider (Vector Builder Inc., IL, USA) to ensure reproducible astrocyte generation for large-scale experiments.

2.3. Differentiation of astrocytes from hiPSC-derived NPCs

Astrocytes were generated from hiPSC-derived NPCs as described previously (Yeon et al., 2021). Briefly, freshly derived NPCs were plated onto Matrigel-coated 6-well culture plates at a density of 3×10^5 cells/cm^2 in NPC culture medium (DMEM/F12 base medium with 1 × N2 and 1 × B27 supplements; Thermo Fisher Scientific) supplemented with 20 ng/mL basic fibroblast growth factor (bFGF) (Prospec, Ness-Ziona, Israel). On the following day, viral transduction was initiated by exposing cells to lentiviral particles with 1 μg/mL polybrene at a multiplicity of infection (MOI) of 1.0 in fresh NPC medium supplemented with 20 ng/mL bFGF. Transduction efficiency was optimized using spin infection methodology, involving centrifugation at 1000×*g* for 1 h at room temperature (RT). After a 16-h viral exposure period, the medium was exchanged with fresh NPC medium supplemented with 2.5 μg/mL doxycycline (DOX) (Takara) to trigger NFIB expression. The addition of DOX established day 0 of the astrocyte differentiation timeline, and all subsequent time points were calculated from this point. DOX treatment was maintained throughout the 14-day study period. On Day 1, the cells were cultured in NPC medium supplemented with 10 ng/mL ciliary neurotrophic factor (CNTF) (PeproTech, NJ, USA) and 10 ng/mL bone morphogenetic protein 4 (BMP4) (PeproTech). On Day 3, the culture medium was switched to commercial astrocyte medium (ScienCell, CA, USA), which was maintained until day 14. Throughout Days 1–14, viral-transduced cells were selected using 1.25 μg/mL puromycin (Thermo Fisher Scientific). On day 14, cells were transferred onto fresh Matrigel-coated culture plates (6-well or 4-well format) at a reduced density of 3×10^4 cells/cm^2 and cultured for an additional week. During this final maturation phase, cells were cultured in specialized astrocyte maturation medium consisting of equal parts DMEM/F12 and Neurobasal media (1:1 ratio) supplemented with 1 × N2, 1 × GlutaMAX™ supplement (Thermo Fisher Scientific), 1 mM sodium pyruvate (Thermo Fisher Scientific), 5 μg/mL heparin-binding epidermal growth factor-like growth factor (PeproTech), 0.5 mg/mL dibutyryl-cAMP (Millipore Sigma), 10 ng/mL BMP4, and 10 ng/mL CNTF. To induce reactive astrocyte activation, day 20 astrocytes were treated with a cytokine mixture consisting of 30 ng/mL TNF-α (Cell Signaling Technology, MA, USA), 3 ng/mL IL-1α (PeproTech), and 400 ng/mL C1q (Millopore Sigma) for 72 h. In select experiments, 1 μM all-*trans* RA (Millipore Sigma) was co-administered with the cytokine mixture.

2.4. Immunocytochemical staining and analysis

Cells cultured on glass coverslips were washed twice with phosphate buffered saline (PBS) and fixed in a 4% paraformaldehyde solution for 15 min at RT. After three washes with PBS, the cells were permeabilized with a 0.1% Triton X-100 solution for 15 min to facilitate antibody penetration into the cytoplasm. Nonspecific binding was blocked using 2% bovine serum albumin in PBS for 1 h at RT. Subsequently, immunostaining was performed overnight at 4 °C with primary antibodies (see below) or phalloidin (Thermo Fisher Scientific). After washing with PBS, the respective Alexa Fluor conjugated secondary antibody (1:1000) (Alexa fluor® 488 or 568; Thermo Fisher Scientific) was applied for 1 h at RT. Coverslips were mounted on glass slides using a 4′, 6-diamidino-2-phenylindole (DAPI)-containing mounting solution (Vector Laboratories, CA, USA) and images were captured using a fluorescence microscope (IX71) equipped with a digital camera (DP71) (both from Olympus). Primary antibodies used in this study were as follows: GFAP (1:1000; Z0334, Agilent, CA, USA), S100β (1:1000; S2532, Millipore Sigma), CD44 (1:100; MA4400, Thermo Fisher Scientific), MAP2 (1:1000; MAB3418, Thermo Fisher Scientific), cleaved caspase 3 (1:1000; 9661, Thermo Fisher Scientific). Image analysis was performed using the ImageJ software (National Institutes of Health, MD, USA). Quantitative analysis of the astrocyte surface was performed to measure the area and intensity of positive signals corresponding to phalloidin and CD44. These values were then divided by the number of cells to determine the average cell area and fluorescence intensity per microscopic field.

2.5. RNA isolation and real-time PCR

RNA extraction was carried out using TRIzol (Thermo Fisher Scientific) according to the manufacturer's instructions. Reverse transcription was performed on 1 μg of total RNA using PrimeScript RT Master Mix (Takara). Gene expression analysis was conducted via quantitative PCR (qPCR) using the SYBR Green Master Mix (Thermo Fisher Scientific) on a StepOnePlus Real-Time PCR System (Thermo Fisher Scientific). Expression levels were calculated using the $2^{-\Delta\Delta Ct}$ method, with Ct representing the threshold cycle value. Target gene Ct values were normalized against ribosomal protein S18 (RPS18) as the reference gene. Results were expressed as relative expression levels comparing experimental samples to control samples. Primer sequences for all analyzed genes are provided in Table S1.

2.6. Glutamate uptake assay

For glutamate uptake assessment, the cells were rinsed twice with HBSS (Thermo Fisher Scientific) and then exposed to 100 μM glutamate in HBSS for 2 h. After the incubation period, the medium from the samples was harvested and glutamate levels were measured using a glutamate assay kit (Abcam, Cambridge, UK), following the provided protocol.

2.7. Synaptosome uptake assay

Synaptosome extraction was performed from the hippocampal tissue of postnatal day 1 mice using the Syn-PER® Synaptic Protein Extraction Reagent (Thermo Fisher Scientific) and labeled with the pHrodo™ Red Microscale Labeling Kit (Thermo Fisher Scientific) according to the manufacturer's instructions. The pHrodo-labeled synaptosomes (0.35 μL) were added to astrocyte and incubated for 24 h. Following the incubation period, random field imaging was conducted with a minimum of five images captured per well across 4-well plates, using the same method as for immunocytochemical analysis. Phagocytic activity was quantified by measuring the area occupied by pHrodo-positive signals and normalized to cell density.

2.8. Nitric oxide assay

Nitric oxide (NO) production was measured in culture media using a colorimetric NO assay kit (Abcam), according to the manufacturer's instructions. Briefly, astrocytes were treated under various experimental conditions. At the end point, conditioned media were collected and centrifuged at 1000×*g* for 10 min at 4 °C to remove cellular debris. The supernatants were then stored at −80 °C until analysis. NO measurement was performed by mixing 85 μL of each sample with 5 μL of nitrate reductase and 5 μL of enzyme cofactor in a 96-well plate. The mixture was incubated at RT for 1 h to convert the nitrate to nitrite. Subsequently, 5 μL of Enhancer was added, followed by incubation at RT for 10 min. Finally, 50 μL of Griess Reagent R1 and R2 each were sequentially added. Using a microplate reader (HIDEX, Turku, Finland), absorbance was measured at 540 nm.

2.9. Enzyme-linked immunosorbent assay (ELISA) for measuring RA

A Human Retinoic Acid Kit (MyBioSource, CA, USA) was used to measure the amount of RA in astrocytes. Adherent cells were detached by treatment with Accutase (Thermo Fisher Scientific) and resuspended. The cell suspension was subjected to three freeze-thaw cycles in liquid nitrogen to achieve homogenization. Cells were then centrifuged at maximum speed for 5 min at 4 °C, and the supernatant was collected and transferred to a clean tube. The subsequent procedures were performed in accordance with the manufacturer's instructions.

2.10. Cytokine beads array

The LEGENDplex Pre-defined Panel (Human Inflammation Panel 1) (BioLegend, CA, USA) was used to measure the levels of cytokines in the conditioned media. The astrocyte-conditioned medium was collected and centrifuged at 1000×*g* for 10 min at 4 °C to remove cellular debris. The subsequent procedures were performed according to the manufacturer's instructions.

2.11. Measurement of mitochondrial membrane potential

Mitochondrial membrane potential was evaluated using JC-1 dye (MedChemExpress). The suspended cells were treated with 2 μM JC-1 in astrocyte maturation medium and incubated at 37 °C for 15 min. Following a single wash step, the cells were resuspended in PBS and analyzed by a FACSymphony A1 (BD Biosciences, NJ, USA) instrument, with 10,000 events recorded for each experimental condition.

2.12. Analysis of mitochondrial morphology

Live-cell mitochondrial morphology was assessed using MitoTracker™ (Thermo Fisher Scientific) staining. A working solution containing 200 nM MitoTracker™ in astrocyte maturation medium was prepared and prewarmed to 37 °C. After removing existing medium from 4-well plate cultures, the cells were incubated with the staining solution for 45 min at 37 °C. Following incubation, cells were washed and maintained in fresh prewarmed maturation medium for imaging. Fluorescence microscopy images were captured using the same method as for immunocytochemical analysis. Image analysis involved cellular segmentation followed by Mitochondria Analyzer plugin within ImageJ-Fiji (National Institutes of Health).

2.13. Assessment of mitophagy activity

NPCs were co-infected with lentivirus expressing the mito-SRAI mitophagy probe according to the astrocyte differentiation protocol. Day 20 astrocytes were treated under various experimental conditions. On day 23, astrocytes were detached using Accutase and resuspended in PBS for analysis. Astrocytes were analyzed by flow cytometry using the FACSymphony A1 instrument to measure mitophagy. The mitophagy index was determined by gating a population with low YPET fluorescence relative to that of TOLLES.

2.14. Western blotting

Cell lysates were obtained from astrocytes using RIPA lysis buffer supplemented with a cocktail of protease and phosphatase inhibitors. Equal amounts of protein (20 μg) were separated on 8% Bis-Tris polyacrylamide gels using NuPAGE MES SDS running buffer (Thermo Fisher Scientific) and transferred onto polyvinylidene fluoride membranes (Millipore Sigma) using a Mini-PROTEAN III apparatus (Bio-Rad). The membranes were then incubated with the anti-phospho-ERK (1:1000; 4370T, Thermo Fisher Scientific), anti-ERK (1:1000; 4695T, Thermo Fisher Scientific), anti-phospho-p38 (1:1000; 4511T, Thermo Fisher Scientific), anti-p38 (1:1000; 8690T, Thermo Fisher Scientific), anti-phospho-p65 (1:1000; 3033s, Thermo Fisher Scientific), anti-p65 (1:1000; ab16502, Thermo Fisher Scientific), anti-phospho-JNK (1:1000; AP0631, ABclonal, MA, USA), anti-JNK (1:1000; A4867, ABclonal) and anti-β-actin (1:1000; sc-7210, Santa Cruz Biotechnology, TX, USA) primary antibodies. After washing, the membranes were incubated with horseradish peroxidase-conjugated anti-mouse Immunoglobulin G (1:2000; 7076s, Cell Signaling Technology) and horseradish peroxidase-conjugated anti-rabbit Immunoglobulin G (1:2000; sc-2357, Santa Cruz Biotechnology) secondary antibodies. Enhanced chemiluminescence was used to detect protein bands (Thermo Fisher Scientific).

2.15. NF-κB reporter assay

Lentiviral reporter constructs were used to assess NF-κB pathway activation. These reporters contained an EGFP fluorescent protein driven by a minimal CMV promoter (mCMV) containing four consecutive NF-κB transcriptional response elements with the sequence motif 5′-GGGACTTTCC. The reporter system also included a PGK_mRuby3 cassette for constitutive mRuby3 expression, which served as an internal control to correct for cell size and infection efficiency. Flow cytometric analysis of EGFP fluorescence was performed using a FACSymphony A1 system.

2.16. Differentiation of hiPSC-derived neurons and co-culture with hiPSC-derived astrocytes

Neuronal differentiation of hiPSC-derived NPCs was achieved through Ngn2 overexpression using an established protocol with slight adaptations (Ho et al., 2016). Briefly, NPCs were seeded at 3×10^5 cells/cm^2 on Matrigel-coated 6-well plates using NPC medium supplemented with 20 ng/mL bFGF. Twenty-four hours after seeding, cells underwent viral transduction with Ngn2 lentivirus (MOI 1.0) in the presence of 1 μg/mL polybrene using fresh NPC medium containing 20 ng/mL bFGF for 18 h. The viral medium was then aspirated and replaced with conversion medium 1 (DMEM/F12 with 1 × N2 and 1 × NEAA) supplemented with 10 ng/mL brain-derived neurotrophic factor (BDNF) (Prospec), 10 ng/mL glial cell line-derived neurotrophic factor (GDNF) (Prospec), and 2.5 μg/mL DOX for Ngn2 expression induction. The addition of DOX marked day 0 of differentiation. Beginning on day 1, cells were maintained in conversion medium 2 (Neurobasal medium with 1 × B27 and 1 × GlutaMAX™) with the addition of 10 ng/mL BDNF, 10 ng/mL GDNF, 2.5 μg/mL DOX, and 1.25 μg/mL puromycin. Puromycin selection was performed from days 1–4, and on day 4, the cells were reseeded onto 4-well plates pre-seeded with hiPSC-derived astrocytes (5×10^4 cells/cm^2) at a final neuronal density of 1×10^5 cells/cm^2 to establish co-cultures. Following co-culture establishment, the cells were treated with either TIC or RA and maintained for an additional 5 days in conversion medium 2 without BDNF, GDNF, DOX, or puromycin.

2.17. Statistical analyses

Each experimental condition was repeated at least three times independently, with data reported as mean ± standard deviation. The Student's *t*-test was used for pairwise comparisons, whereas two-way analysis of variance was employed for multiple group comparisons. A significance threshold of $p < 0.05$ was applied across all statistical tests.

3. Results

3.1. Inflammatory cytokine cocktail induces functional and molecular alterations related to reactivity in hiPSC-Derived astrocytes

We previously developed a reliable *in vitro* model using hiPSC-derived astrocytes to establish a cellular platform for investigating

human-specific astrocyte biology (Yeon et al., 2021). The overexpression of NFIB, a transcription factor critical for astrocyte development, in hiPSC-derived NPCs generated a highly enriched population of astrocytes within 3 weeks (Fig. S1). Immunocytochemical analysis followed by quantification revealed that the majority of cells were positive for GFAP, S100β, and CD44 at more than 90% of efficiency (Fig. S1A–B). Treatment with TIC for 3 days induced marked morphological changes, characterized by enlarged somata and blunt processes, which are features commonly associated with reactive astrocytes exhibiting an inflammatory phenotype (Li et al., 2020) (Fig. 1A). Notably, CD44 expression is frequently elevated in reactive astrocytes and is implicated in exacerbated inflammatory responses across various neurological disorders (Cargill et al., 2012; Kruk et al., 2023). Immunoreactivity for CD44 was significantly intensified in TIC-treated cells than that in untreated controls, corroborating the morphological observations (Fig. 1B).

One of the hallmarks of reactive astrocytes is their distinct gene expression profile, with a prominent upregulation of genes associated with inflammation. Accordingly, qPCR revealed a transcriptional signature consistent with the previously defined markers of astrocyte reactivity (Liddelow et al., 2017). Lipocalin2 (*LCN2*), tissue inhibitor of metalloproteinase 1 (*TIMP1*), *CD44* and complement component 3 (*C3*), which are general markers of astrocyte activation in various diseases, were robustly upregulated. Additionally, expression of serglycin (*SRGN*), and proteasome subunit beta 8 (*PSMB8*), FK506 binding protein (*FKBP5*), and serine protease inhibitor family G Member 1 (*SERPING1)* was significantly increased by TIC treatment compared to that in controls. These genes are commonly associated with the "A1-like phenotype" of reactive astrocytes, which has been linked to detrimental effects on neuronal survival and synaptic function (Liddelow et al., 2017). Inflammatory cytokines, *IL6* and *IL8*, were also upregulated, further supporting the inflammatory profile of these reactive astrocytes (Fig. 1C).

Functional assays further confirmed the acquisition of reactive properties and revealed notable deficits in TIC-treated astrocytes. Glutamate uptake was significantly impaired in TIC-treated astrocytes, indicating a diminished capacity to clear primary excitatory neurotransmitters (Fig. 1D). Similarly, TIC treatment reduced the phagocytic capacity of astrocytes, as shown by the decreased uptake of pHrodo-labeled mouse brain-derived synaptosomes (Fig. 1E and Fig. S2), indicating a compromised ability to clear synaptic debris. Inflammatory stimuli often drive astrocytes to upregulate the expression of inducible nitric oxide synthase (*iNOS*), leading to increased NO production. Although NO serves important signaling functions at low levels, excessive NO is cytotoxic, damages DNA, proteins, and lipids, and disrupts astrocytic homeostasis (Wang et al., 2015). We observed a significant upregulation of *iNOS* transcription and enhanced NO production in TIC-treated astrocytes compared to that in the untreated control (Fig. 1F–G). As excessive NO production is associated with astrocyte-mediated neurotoxicity (Wang et al., 2015), this outcome serves as a valuable indicator for evaluating the pathological potential of reactive astrocytes and therapeutic interventions.

Collectively, these findings demonstrate that our hiPSC-derived astrocyte model recapitulated the key morphological, functional, and molecular characteristics of reactive astrocytes. In this study, we use the term "inflammatory reactivity" to describe the cells' phenotype as previously proposed (Leng et al., 2022), to more accurately reflect our focus on the inflammation-related phenotypes of these cells.

3.2. RA metabolic pathway is altered in TIC-induced reactive astrocytes

Previous studies using animal models and *in vitro* systems have shown that RA has context-dependent regulatory effects on inflammatory responses mediated by astrocytes (Mizee et al., 2014; van Neerven et al., 2010). However, studying the precise actions of RA in human CNS inflammation has been difficult because of the lack of physiologically relevant model systems. Thus, we utilized a hiPSC-derived astrocyte model to investigate the effects of astrocyte activation on RA metabolism, with a particular focus on the expression patterns of key enzymes involved in the biosynthetic pathway (Fig. 2A). To begin, we examined the expression of the genes encoding these enzymes.

Quantitative gene expression analysis demonstrated that astrocytes treated with TIC exhibited a marked reduction in the expression of enzymes involved in RA biosynthesis. Specifically, the expression of *ALDH1A1, ALDH1A2*, and *ALDH1A3* was significantly decreased after TIC treatment (Fig. 2B). In contrast, the expression levels of the upstream enzymes, *RDH10* and *DHRS9*, which catalyze the initial oxidation of retinol to retinaldehyde, remained unchanged (Fig. 2C). This indicates that, while the capacity to convert retinol to retinaldehyde is retained, the final step of RA synthesis, the conversion of retinaldehyde to RA, is altered in TIC-treated astrocytes. The coordinated downregulation of all three *ALDH1A* subtypes suggests that this is not a random effect, but a part of a regulated response associated with astrocyte activation. Among the enzymes that catalyze the reduction of retinaldehyde to retinol, *DHRS13* was significantly upregulated, whereas *DHRS3* expression was significantly downregulated by TIC treatment (Fig. 2D). However, since both enzymes perform the same catalytic function, opposing changes in their expression levels are likely to result in no net change in the overall capacity for retinaldehyde-to-retinol conversion. Notably, *CYP26A1* showed no significant changes in expression (Fig. 2E), suggesting that TIC may not alter the intrinsic RA-degrading capacity of astrocytes. Once synthesized, RA is sequestered by cellular retinoid-binding proteins (CRABPs), including CRABP1 and CRABP2, that regulate its subcellular distribution and signaling pathways. CRABP1 facilitates the delivery of RA to CYP26A1 for metabolic degradation, whereas CRABP2 transports RA into the nucleus for RAR/RXR-mediated transcriptional activation (Napoli, 2017). TIC treatment resulted in the differential regulation of these binding proteins, with significantly decreased *CRABP1* expression and significantly increased *CRABP2* expression (Fig. 2F). The concurrent downregulation of *CRABP1* and upregulation of *CRABP2* suggested a coordinated shift in RA handling, potentially reducing RA degradation while enhancing its nuclear delivery and transcriptional activity as a compensatory mechanism to maximize the utilization of limited RA availability.

Subsequently, we examined publicly available RNA sequencing datasets (GSE182307) and compared the transcriptomic profiles of hPSC-derived astrocytes with and without TIC treatment to validate these findings (Leng et al., 2022). Consistent with our results, the genes encoding RA-synthesizing enzymes (*ALDH1A1, ALDH1A2, ALDH1A3*) were found to be downregulated in TIC-treated astrocytes (Fig. S3A–B). Gene set enrichment analysis also revealed similar trends, showing the downregulation of genes involved in RA synthesis and the upregulation of genes involved in RA degradation (Fig. S3C–D). Finally, direct measurement of RA levels by ELISA confirmed a significant reduction in intracellular RA in TIC-treated astrocytes compared to that in controls (Fig. 2G). Together, these findings suggested that TIC-mediated reactivity induced the coordinated suppression of RA biosynthesis in astrocytes, while modulating retinoid metabolism at multiple levels. The active suppression of RA availability represents a novel regulatory mechanism that highlights the potential importance of RA metabolism in shaping reactive astrocyte phenotypes.

3.3. RA supplementation suppresses inflammatory gene expression

Based on the dysregulation of RA biosynthesis in TIC-induced reactive astrocyte models we investigated whether exogenous RA supplementation modifies their inflammatory reactivity. This approach may also clarify whether the reduction in RA levels was simply a downstream consequence of astrocyte activation or whether it functionally contributed to sustaining the reactive phenotype.

Our results demonstrated that co-treatment with 1 μM RA and TIC downregulated the levels of key pro-inflammatory cytokines, including IL-6 and IL-8, which were upregulated by TIC (Fig. 1C) at the mRNA and

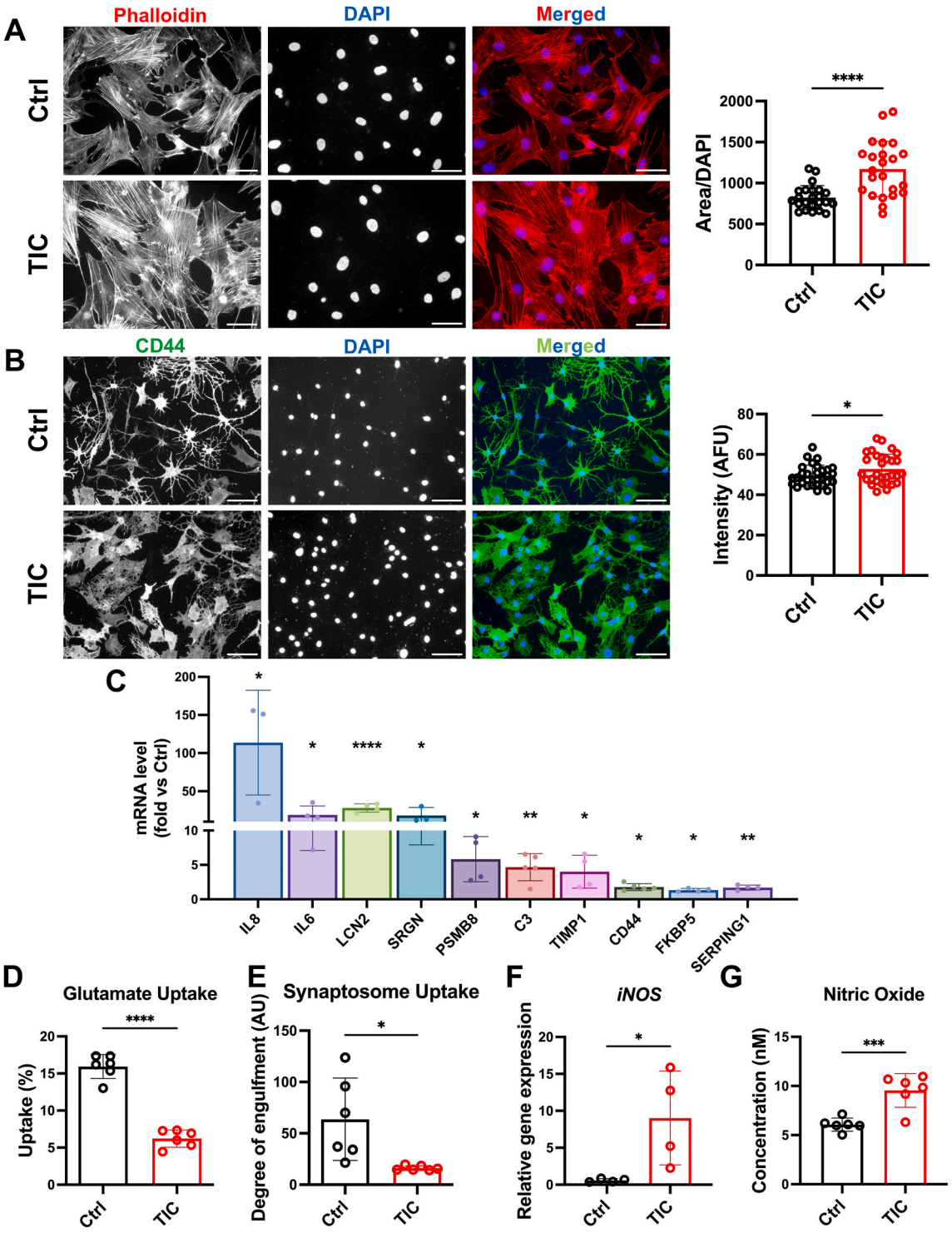

Fig. 1. Inflammatory cytokine cocktail induces functional and molecular alteration related to reactivity in iPSC-derived astrocytes

A. Representative immunofluorescence images showing phalloidin (red) and DAPI (blue) staining in control (Ctrl) and TIC-treated astrocytes. Quantification of phalloidin-positive area per DAPI-positive cell shows significant increase in TIC-treated group. Quantitative analysis was based on immunofluorescent images from three independent experiments. Scale bars, 30 μm. **B.** CD44 immunofluorescence (green) with DAPI (blue) in control and TIC-treated astrocytes. Quantification demonstrates increased CD44 intensity in TIC-treated cells compared to controls. The quantification was conducted on immunofluorescent images from three independent experiments. AFU: Arbitrary Fluorescence Units. Scale bars, 60 μm. **C.** mRNA expression levels of astrocyte reactivity markers measured by quantitative PCR (qPCR). All genes tested show significant upregulation in TIC-treated cells compared to control ones. **D.** Glutamate uptake assay showing reduced glutamate uptake capacity in TIC-treated astrocytes compared to controls. **E.** Synaptosome engulfment assay demonstrating reduced capacity in TIC-treated astrocytes. **F.** *iNOS* expression levels showing upregulation in TIC treatment. **G.** Nitric oxide (NO) assay showing significantly increased NO production in TIC-treated astrocytes. *p* value was determined by two-tailed unpaired *t*-test (A-G). $*p < 0.05$, $**p < 0.01$, $***p < 0.001$, $****p < 0.0001$.

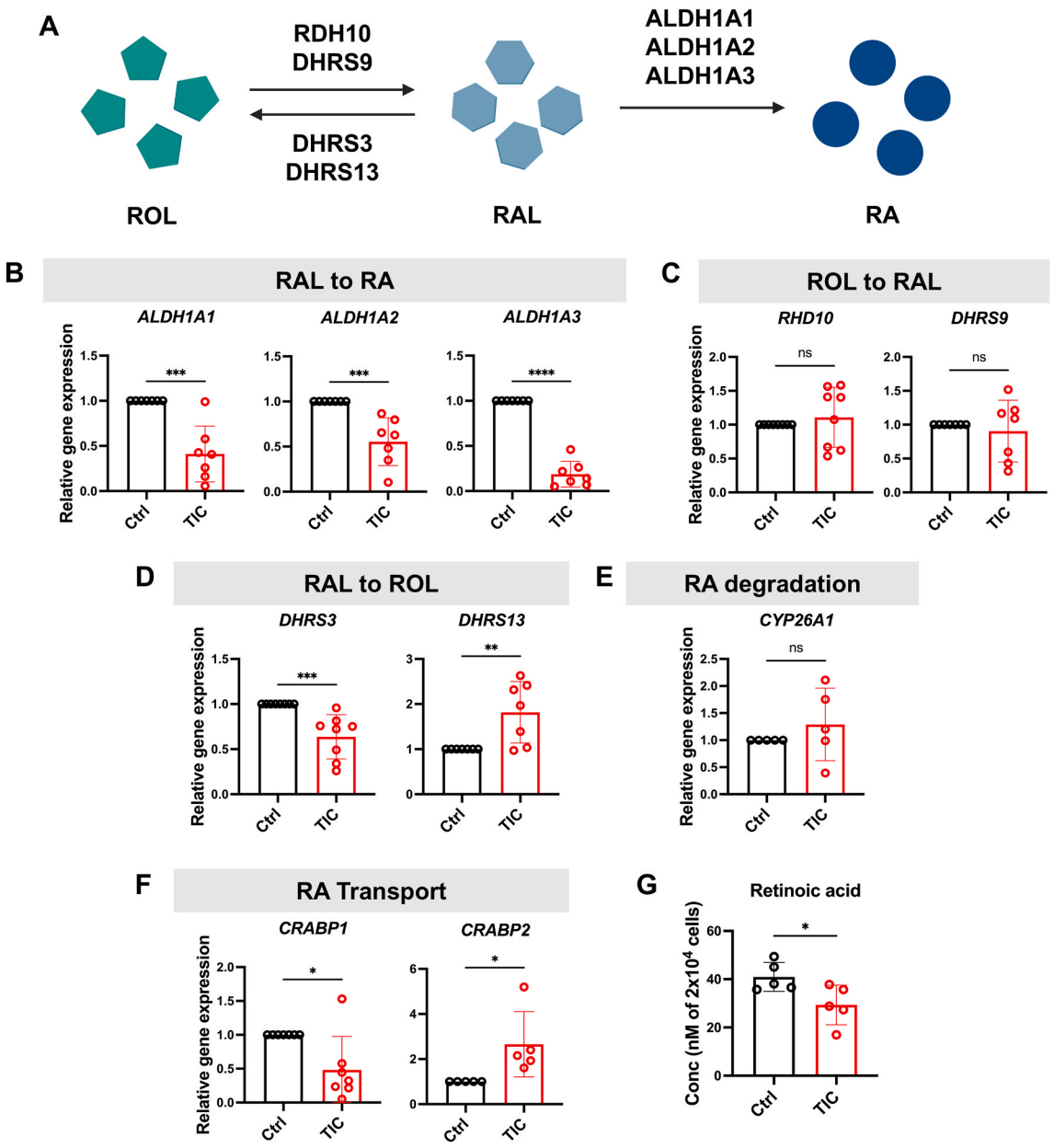

Fig. 2. RA metabolic pathway is altered in reactive astrocytes

A. Schematic diagram of retinoic acid (RA) metabolic pathway showing conversion from retinol (ROL) to retinaldehyde (RAL) to RA, with key enzymes: RDH10/DHRS9 (ROL to RAL), DHRS3/DHRS13 (RAL to ROL), and ALDH1A1/1A2/1A3 (RAL to RA). **(B–F)** Quantitative gene expression analysis of RA metabolic enzymes. Data were obtained from five to eight batches of differentiation. Data are expressed as fold changes relative to control, calculated using the $2^{-\Delta\Delta Ct}$ method with RPS18 as a reference gene. **G.** RA concentration measurements in cell lysates show decreased RA levels in TIC-treated cells. *p* value was determined by two-tailed unpaired *t*-test (B-G). ns: not significant, $*p < 0.05$, $**p < 0.01$, $***p < 0.001$, $****p < 0.0001$.

protein levels (Fig. 3A–B). NF-κB is a master transcriptional regulator of inflammatory gene expression and is activated by various inflammatory stimuli including the cytokines used in our treatment (Liu et al., 2017). RA supplementation markedly suppressed the phosphorylation of p65, a key regulatory subunit of the NF-κB complex (Fig. 3C, Fig. S4). Consistent with this, results of the NF-κB reporter assay showed that RA significantly reduced TIC-induced transcriptional activity of NF-κB, indicating that RA inhibits NF-κB-mediated gene transcription (Fig. 3D). Treatment of astrocytes with RA alone did not significantly affect the expression of pro-inflammatory markers or the phosphorylation of NF-κB (Fig. 3B–D). Together, these findings suggest that RA suppresses pro-inflammatory responses from TICs by inhibiting the NF-κB signaling pathway and its downstream targets.

Notably, TIC treatment also increased the expression of anti-inflammatory cytokines such as *IL10* and *TGFβ* at the transcript level (Fig. 3E). While this may appear contradictory to earlier studies reporting the selective induction of pro-inflammatory genes by TIC (Liddelow et al., 2017), these results are consistent with more recent evidence from human astrocyte models which supports the concurrent upregulation of anti-inflammatory mediators in response to such stimulation (Hyvarinen et al., 2019). Moreover, co-treatment with RA normalized the elevated levels of *IL10* and *TGFβ* (Fig. 3E). Similar to the pro-inflammatory response, astrocyte treatment with RA alone did not significantly affect the expression of anti-inflammatory mediators. These findings indicate that RA attenuates the pro-inflammatory and anti-inflammatory responses in reactive astrocytes, which suggests that RA does not simply shift astrocytes toward an anti-inflammatory phenotype but rather dampens the key inflammatory transcriptional

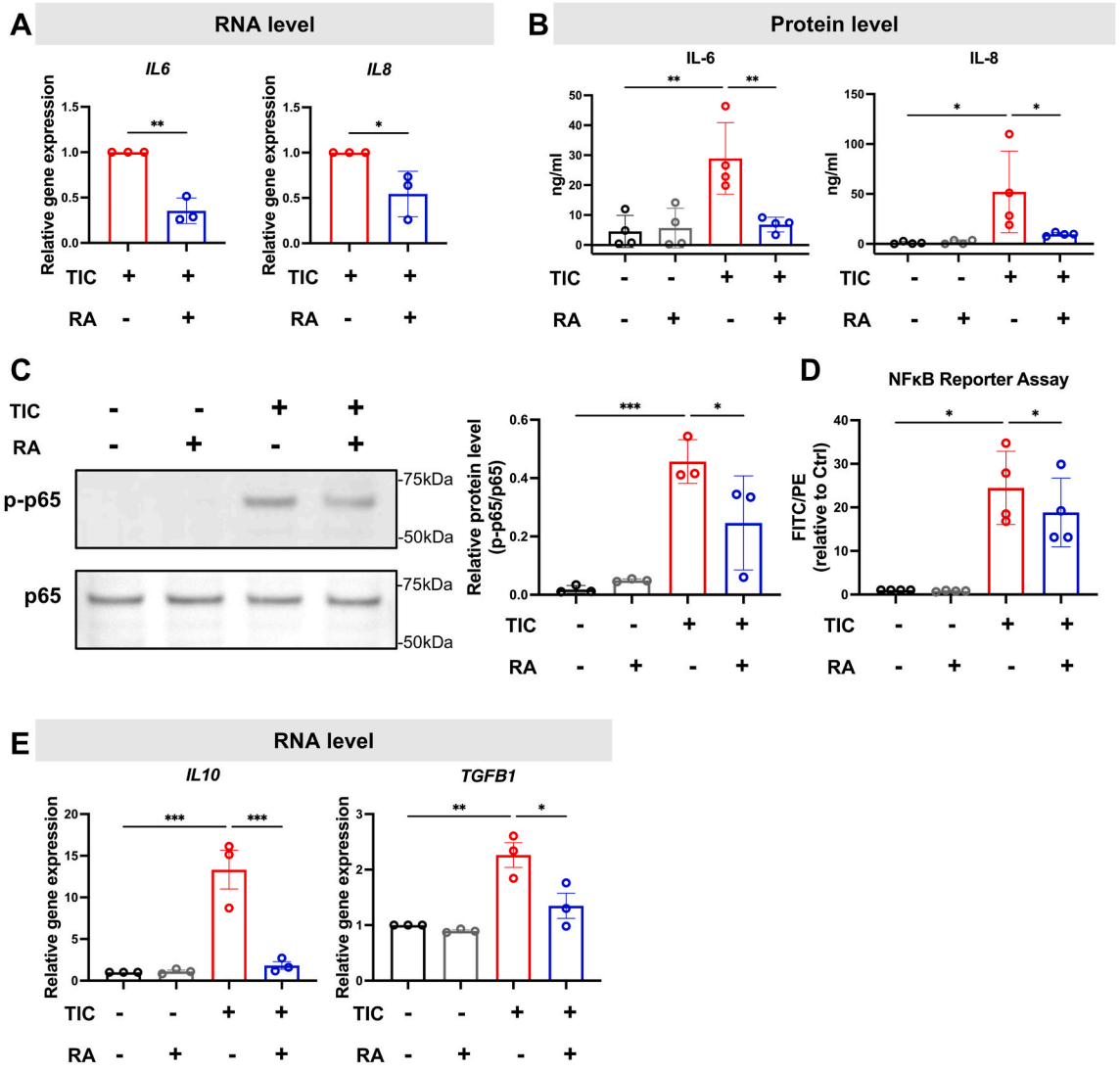

Fig. 3. RA supplementation suppresses inflammatory gene expression
A. Expressions of the pro-inflammatory cytokines *IL6* and *IL8* were significantly reduced by RA treatment. **B.** Cytokine beads array for IL-6 and IL-8 protein levels in culture supernatants. RA treatment reduced cytokine secretion. **C.** Representative Western blot images and the results of densitometric quantification of phospho-p65 (p-p65) and total p65. RA treatment reduced TIC-induced NFκB activation. The protein samples were obtained from three independent differentiations. **D.** NFκB transcriptional activity measured by reporter assay, confirming reduced NFκB activity with RA treatment. **E.** Relative gene expression of anti-inflammatory cytokines *IL10* and *TGFβ* in presence of TIC and/or RA. *p* value was determined by two-tailed unpaired *t*-test (A) or two-way repeated measures (RM) ANOVA with Tukey's post-hoc test (B–D). $*p < 0.05$, $**p < 0.01$, $***p < 0.001$.

program.

3.4. *RA selectively modulates stress-related signaling pathways in reactive astrocytes induced by TIC*

Next, we sought to elucidate the molecular mechanism underlying inflammation-suppressing effects of RA on reactive astrocytes. We first explored whether RA exerts its effects by directly regulating target gene expression through the RAR/RXR complex. We used AGN193109, the pan-RAR antagonist, in combination with TIC and RA. Notably, co-treatment with AGN193109 did not significantly reverse the inhibitory effect of RA on the expression of any of the cytokines tested (Fig. S5). This suggests that the anti-inflammatory actions of RA in reactive astrocytes may occur via RAR-independent mechanisms or alternative signaling pathways. To explore this possibility, we then focused on stress-related signaling pathways previously implicated in RA action (Chatterjee and Chatterji, 2017; Xin et al., 2025; Yen et al., 1998; Zhang et al., 2018; Zhou et al., 1999). Specifically, we examined the phosphorylation status of three key MAPK pathways—ERK, p38 MAPK, and JNK—under the co-treatment condition. As shown in Fig. 4, Western blot analysis revealed that TIC treatment significantly increased ERK and p38 MAPK phosphorylation, whereas JNK phosphorylation remained unchanged. These findings suggest that ERK and p38 MAPK, but not JNK, are selectively activated in astrocytic inflammatory responses triggered by TIC (Fig. 4A–D, Fig. S6). Co-treatment with RA under the same conditions resulted in a significant reduction in the phosphorylation of ERK and p38 MAPK (Fig. 4A–C). This selective inhibition of MAPK signaling by RA is relevant to our previous observations that RA attenuates TIC-induced phosphorylation and transcriptional activity of NF-κB (Fig. 3C–D). Previous studies demonstrated that ERK can enhance the IKK complex, promoting IκBα degradation and subsequent nuclear translocation of NF-κB (Vanden Berghe et al., 1998) and that p38 MAPK facilitates NF-κB transactivation via mitogen-and stress-activated protein kinase-1-dependent phosphorylation of the p65 subunit (Vanden Berghe et al., 1998; Vermeulen et al., 2003). Therefore, the RA-induced suppression of ERK and p38 MAPK

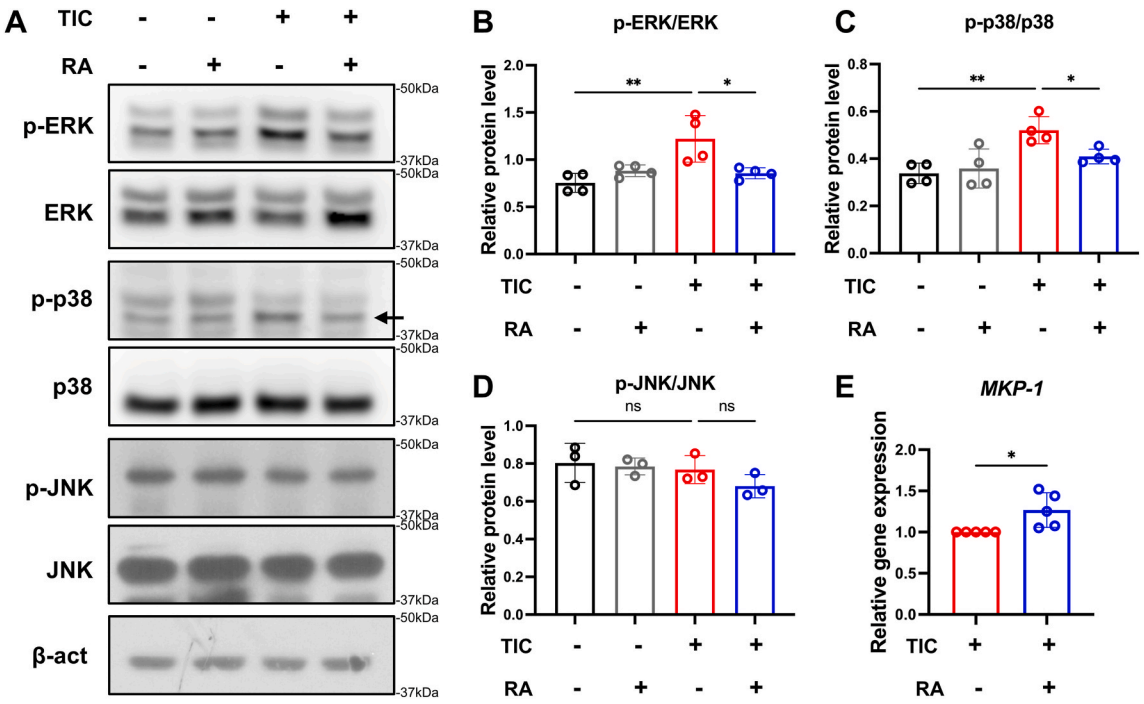

Fig. 4. RA selectively modulates MAPK pathways in TIC-induced reactive astrocytes
A. Western blot analysis of MAPK signaling pathways. Representative images show phosphorylated and total protein levels of ERK, p38 MAPK and JNK with β-act as loading control. **B.** Phospho-ERK (p-ERK)/ERK ratio: Quantification shows RA treatment significantly reduces TIC-induced ERK phosphorylation. **C.** Phospho-p38 (p-p38)/p38 ratio: Quantification shows RA treatment significantly reduces TIC-induced p38 phosphorylation. **D.** Phospho-JNK (p-JNK)/JNK ratio: No significant changes were observed across the treatments. The protein samples were obtained from three or four independent differentiations. **E.** RA treatment significantly increased the relative gene expression of *MKP-1* in TIC-treated astrocytes. *p* value was determined by two-way RM ANOVA with Tukey's post-hoc test (B-D) or two-tailed unpaired *t*-test (E). ns: not significant, $*p < 0.05$, $**p < 0.01$.

phosphorylation may have likely contributed to the decreased activation of NF-κB observed in previous experiments. To further investigate the possible mechanism by which RA restores the phosphorylation status of ERK and p38 MAPKs specifically in the presence of TIC, we examined the expression of MAPK phosphatase-1 (MKP-1), a dual-specificity phosphatase that is known to negatively regulate MAPK signaling by dephosphorylating ERK and p38 MAPK. Quantitative gene expression analysis revealed that RA treatment significantly upregulated *MKP-1* expression in TIC-induced reactive astrocytes (Fig. 4E). This result suggests that the observed reduction in ERK and p38 MAPK phosphorylation may be mediated, at least in part, by enhanced *MKP-1* expression.

Taken together, our data support a model in which RA suppresses astrocytic inflammatory reactivity by targeting the ERK and p38 MAPK pathways, thereby attenuating the activation of the downstream transcription machinery. This signaling interference ultimately leads to reduced expression of pro- and anti-inflammatory cytokines, including *IL6, IL8, IL10,* and *TGFβ*, in reactive astrocytes.

3.5. RA treatment suppresses negative effect of reactive astrocytes on neuronal survival

Subsequently, we examined whether RA suppressed other pathological features of reactive astrocytes. As we previously observed increased production of NO, a known mediator of reactive astrocyte-mediated neurotoxicity (Wang et al., 2015) (Fig. 1F–G), we co-cultured astrocytes with hiPSC-derived neurons in the presence or absence of TIC and/or RA for 72 h. Neither TIC nor RA alone significantly affected neuronal viability when not in co-culture with astrocytes, as shown by cleaved caspase 3 (CC3) immunostaining (Fig. S7). However, neurons co-cultured with astrocytes in the presence of TIC exhibited a marked increase in CC3-positive cells, indicating enhanced neuronal death, consistent with previous reports (Barbar et al., 2020) (Fig. 5A–B). Notably, co-culturing with astrocytes in the presence of TIC and RA substantially reduced the number of CC3-positive neurons, restoring them to near control levels (Fig. 5A–B). To investigate the potential mechanistic link, we examined the effects of RA on NO production. We found that RA treatment downregulated *iNOS* transcript levels and reduced NO levels in the culture medium (Fig. 5C–D). Although the precise mechanism by which RA suppresses the negative effects of TIC-induced reactive astrocytes on neuronal survival requires further investigation, the inhibition of NO production may be a contributing factor. Collectively, our findings demonstrate that RA treatment effectively reverses the inflammatory state of astrocytes and restores their homeostatic functions. This highlights RA's potential as a promising multi-target therapeutic agent for treating CNS diseases characterized by reactive astrogliosis.

3.6. RA supplementation restores altered mitochondrial morphology and function by TIC

In TIC-treated astrocytes, NO production was significantly increased (Fig. 1G). Since NO is also a well-established mediator linking astrocyte reactivity to mitochondrial collapse in neuroinflammatory models (Ghasemi et al., 2018; Stewart and Heales, 2003), we hypothesized that the observed neurotoxicity might coincide with mitochondrial compromise in astrocytes. We therefore evaluated potential alterations in mitochondrial function and morphology.

To assess mitochondrial structure, we used confocal microscopy with MitoTracker™ staining. As expected, astrocytes treated with TIC exhibited pronounced mitochondrial fragmentation. This was quantitatively confirmed by significant reductions in both the mean aspect ratio (reflecting elongation) and the mean form factor (reflecting branching complexity), compared to untreated controls (Fig. 6A–B).

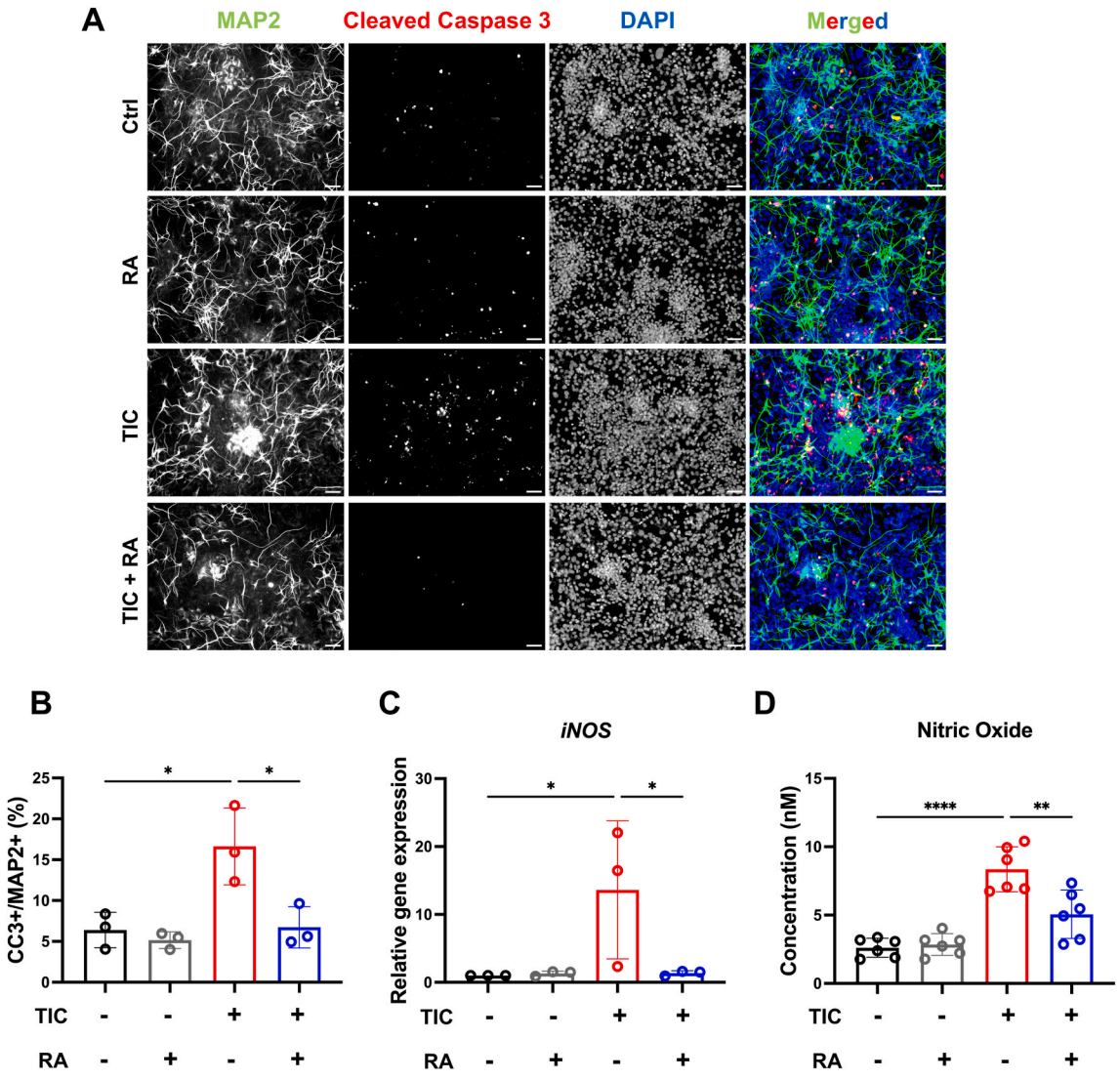

Fig. 5. RA treatment suppresses negative effect of reactive astrocytes on neuronal survival
A. Representative immunofluorescence images showing staining for MAP2 (green), cleaved caspase 3 (CC3) (red) and DAPI (blue) in a co-culture of neurons and astrocytes. Scale bars, 30 μm. **B.** Quantification of CC3-positive cell among MAP2-positive cell shows a significant increase in the TIC-treated group and a significant reduction in the group co-treated with TIC and RA. **C.** *iNOS* gene expression. RA treatment significantly reduces the TIC-induced *iNOS* upregulation. **D.** NO levels in astrocyte culture medium. TIC treatment significantly increased NO production compared to control, while RA co-treatment significantly reduced it. *p* value was determined by two-way RM ANOVA with Tukey's post-hoc test (B-D). $*p < 0.05$, $**p < 0.01$, $****p < 0.0001$.

Notably, co-treatment with RA reversed this TIC-induced fragmentation, restoring the integrity of the mitochondrial network. We then examined mitochondrial membrane potential (MMP), a key indicator of mitochondrial function. Flow cytometric analysis using JC-1 dye showed that TIC treatment significantly reduced MMP, but RA co-treatment restored it to near-control levels (Fig. 6C). This suggests a protective effect of RA on mitochondrial function. In addition to our MMP findings, we observed mitophagy, which is the selective degradation of damaged mitochondria via autophagy and a vital quality control mechanism (Pickles et al., 2018). Mitophagy level, assessed using the pH-sensitive mito-SRAI reporter (Katayama et al., 2020), showed a downward trend in the TIC-treated group compared to the control ($p = 0.055$, One-way ANOVA; Fig. 6D). However, RA co-treatment significantly increased mitophagy level. This indicates that RA helps maintain mitochondrial function and dynamics by preserving quality control activity.

Taken together, our observations suggest that RA helps maintain mitochondrial structural and functional integrity in TIC-induced reactive astrocytes. Further research is necessary to fully elucidate the specific mechanisms by which RA achieves these beneficial effects and how these improvements in mitochondrial health are linked to its broader anti-inflammatory properties.

4. Discussion

Using hiPSC-derived astrocytes in this study was a methodological advancement, as this model reliably reproduces the morphological, molecular, and functional features of reactive astrocytes observed in living organisms. A major finding from this model was the coordinated dysregulation of gene expression related to RA metabolic pathways in reactive astrocytes. This represents the first comprehensive characterization of this process in a human context. We observed significant downregulation of *ALDH1A* family gene expression, suggesting reduced intrinsic RA biosynthetic capacity. Additionally, ELISA confirmed a significant reduction in intracellular RA levels. This alteration appears to remove the anti-inflammatory constraints of RA during the early stage, while simultaneously establishing a persistent RA-limited state that may prolong astrocyte reactivity. Moreover, the functional

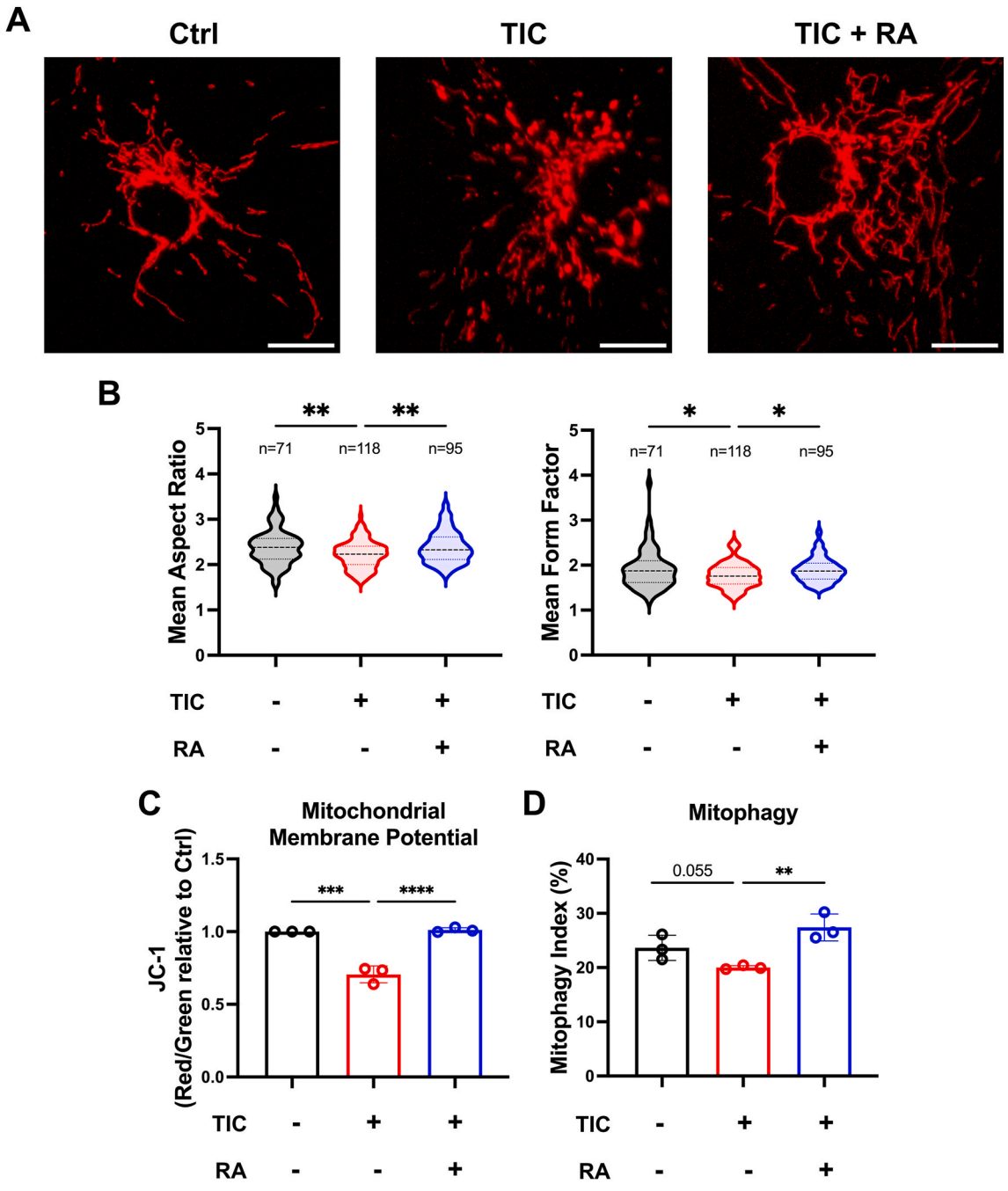

Fig. 6. RA supplementation restores altered mitochondrial morphology and function by TIC
A. Representative images of mitochondrial morphology using MitoTracker™ staining in astrocytes. Scale bars, 10 μm. **B.** Quantification of mitochondrial morphology. TIC treatment significantly reduces both aspect ratio and formed factor, indicating mitochondrial fragmentation. RA treatment restored them. The quantification was conducted on immunofluorescent images from three independent experiments. **C.** Mitochondrial membrane potential (MMP) measurement by JC-1 and flow cytometry. MMP was decreased in TIC-treated astrocytes and restored by RA treatment. **D.** Measurement of mitophagy activity using mito-SRAI. Mitophagy activity was significantly improved by RA treatment in TIC-treated astrocytes. *p* value was determined by one-way RM ANOVA with Tukey's post-hoc test (B-D). $^{*}p < 0.05$, $^{**}p < 0.01$, $^{***}p < 0.001$, $^{****}p < 0.0001$.

importance of the altered RA metabolism became evident after exogenous RA treatment. Mechanistically, this RA supplementation suppressed major inflammatory pathways, such as MAPK–NF–κB signaling, which in turn reversed the upregulation of pro-inflammatory mediators. This may also directly lead to decreased expression of *iNOS* and NO production, which are key inflammatory mediators known to drive neuronal damage (Davis et al., 2005). Interestingly, RA also reduced expression of anti-inflammatory cytokines, *IL10* and *TGFβ*. This simultaneous suppression of pro- and anti-inflammatory mediators may reflect the broader inhibition of astrocyte activation by RA (Medzhitov, 2008). As both cytokine types can be regulated by the MAPK pathway (Arthur and Ley, 2013), the action of RA upstream of these pathways could explain the simultaneous reduction.

Our pathway analysis revealed selective modulation of MAPK subfamilies by RA. RA treatment potently suppressed p38 MAPK and ERK activation while sparing JNK activity, which is essential for stress adaptation and cell survival (Davis, 2000). This selective regulation suggests that RA limits pathological signaling while preserving the

necessary cellular responses. The upregulation of *MKP*-1 by RA treatment offers a possible mechanism for its suppressive effect on inflammatory signals. As a key negative regulator of MAPK signaling, MKP-1 is known for its role in resolving inflammatory responses in various cell types (Chi et al., 2006; Manetsch et al., 2012). The induction of *MKP*-1 by RA creates an interesting negative regulatory loop that dampens MAPK activation and, consequently, downstream NF-κB signaling (Vanden Berghe et al., 1998). Additionally, we found that RA restored mitochondrial structure, membrane potential loss and significantly rescued mitophagic activity in TIC-induced reactive astrocytes. Given that mitophagy is essential for eliminating damaged mitochondria and preventing excessive reactive oxygen species production, this restoration may represent another neuroprotective mechanism in RA. Based on the multifaceted activities of RA and its intended regulation, we propose its metabolism as a key regulatory node in astrocyte reactivity and suggest its potential therapeutic role in neuroinflammatory conditions, as summarized in Fig. 7.

Overall, these findings have significant therapeutic implications. The discovery that inflammatory reactivity creates a RA-limited environment suggests that chronic neuroinflammatory diseases may be driven, in part, by metabolic alterations. In this regard, disorders like AD and MS, both characterized by persistent astrocyte activation, could benefit from RA supplementation or interventions that restore endogenous RA synthesis. Consistently, previous studies have linked vitamin A deficiency to cognitive decline, and clinical trials have shown modest cognitive benefits from supplementation (Bonnet et al., 2008; Chen et al., 2021; Ding et al., 2008). In MS, where astrocyte-driven glial scarring hinders remyelination (Kamermans et al., 2019), RA may help temper inflammation while preserving reparative functions.

5. Conclusion

Our study identified RA metabolism as a critical regulator of inflammatory reactivity in astrocytes and presents a compelling case for targeting this pathway in neuroinflammatory disorders. We highlighted a previously unrecognized metabolic checkpoint that sustains pathological activation, by demonstrating that reactive astrocytes actively downregulate RA biosynthesis. This insight expands the current understanding of neuroinflammation and underscores the therapeutic potential of metabolic reprogramming strategies for restoring cellular homeostasis.

CRediT authorship contribution statement

Seo Hyun Yoo: Writing – review & editing, Writing – original draft, Visualization, Methodology, Investigation, Formal analysis. **Dongyun Kim:** Writing – review & editing, Visualization, Methodology, Investigation, Formal analysis, Data curation. **Gyu-Bum Yeon:** Writing – review & editing, Methodology, Formal analysis, Data curation, Conceptualization. **Jaeyeon Choi:** Methodology, Investigation. **Jaewook Lee:** Methodology, Investigation. **Dong-Wook Kim:** Resources, Formal analysis. **Hyunggee Kim:** Writing – review & editing, Supervision, Resources, Funding acquisition, Conceptualization. **Dae-Sung Kim:** Writing – review & editing, Writing – original draft, Supervision, Resources, Project administration, Funding acquisition, Conceptualization.

Funding

This work was supported by grants from the National Research

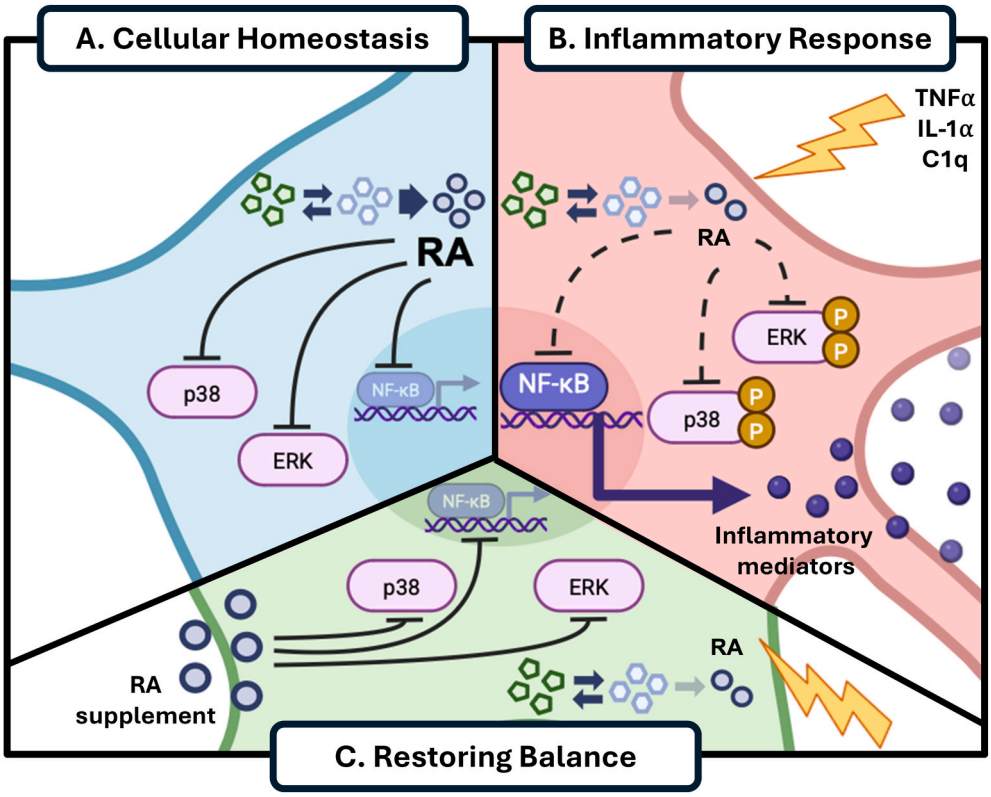

Fig. 7. RA metabolism plays a key regulatory role in the inflammatory reactivity of astrocytes
A. Cellular Homeostasis: Astrocytes maintain a stable balance of RA metabolites, ensuring normal cellular function. **B.** Inflammatory Response: Treatment with TIC disrupts this balance, creating an RA-limited state. This leads to the activation of the MAPK-NFκB signaling pathway, which increases the production of inflammatory mediators. **C.** Restoring Balance: Providing exogenous RA resolves the deficiency, effectively suppressing the inflammatory signaling and production of inflammatory mediators. This action allows the cells to recover their homeostatic functions, including neuroprotection and the maintenance of mitochondrial dynamics.

Foundation of Korea (RS-2023-00218838, RS-2024-00344352), the Korean Fund for Regenerative Medicine (KFRM) grant funded by the Korea government (the Ministry of Science and ICT, the Ministry of Health & Welfare) (24A0101L1), and a research grant from Korea University.

Declaration of competing interest

The authors declare that they have no known competing financial interests or personal relationships that could have appeared to influence the work reported in this paper.

Acknowledgements

The mito-SRAI_pcDNA3 was provided by the RIKEN BRC through the National BioResource Project of the MEXT, Japan. The authors utilized Claude Sonnet 4 (Anthropic) during manuscript preparation to improve language quality, including readability, clarity, and grammar. All AI-generated content was carefully reviewed, revised as necessary, and the authors maintain full accountability for the published article.

List of abbreviations

AD: Alzheimer's disease; ALDH1A: aldehyde dehydrogenase 1A; C1q: complement component 1q; C3: complement component 3; CNS: central nervous system; CRABP: cellular retinoid-binding proteins; CYP26A1: cytochrome P450 26A1; DHRS13: dehydrogenase/reductase 13; DHRS3: dehydrogenase/reductase 3; DHRS9: dehydrogenase/reductase 9; ERK1/2: extracellular signal-regulated kinase 1/2; FKBP5: FK506 binding protein; hiPSCs: human induced pluripotent stem cells; hPSCs: human pluripotent stem cells; IL-10: interleukin-10; IL-1α: interleukin-1α; IL-6: interleukin-6; IL-8: interleukin-8; iNOS: inducible nitric oxide synthase; LCN2: Lipocalin2; MAPK: mitogen activated protein kinase; MKP-1: MAP kinase phosphatase 1; MMP: mitochondrial membrane potential; MOI: multiplicity of infection; MS: multiple sclerosis; NO: nitric oxide; NPCs: neural precursor cells; PBS: phosphate buffered saline; PSMB8: proteasome subunit beta 8; qPCR: quantitative PCR; RA: retinoic acid; RAR: RA receptor; RAREs: RA response elements; RDH10: retinol dehydrogenase 10; RPS18: ribosomal protein S18; RXR: retinoid X receptor; SERPING1: serine protease inhibitor family G Member 1; SRGN: serglycin; TGFβ: Transforming growth factor-beta; TIMP1: tissue inhibitor of metalloproteinase 1; TNF-α: tumor necrosis factor-α.

Appendix A. Supplementary data

Supplementary data to this article can be found online at https://doi.org/10.1016/j.neuint.2026.106134.

References

Alvarez, J.I., Katayama, T., Prat, A., 2013. Glial influence on the blood brain barrier. Glia 61 (12), 1939–1958. https://doi.org/10.1002/glia.22575.

Arthur, J.S., Ley, S.C., 2013. Mitogen-activated protein kinases in innate immunity. Nat. Rev. Immunol. 13 (9), 679–692. https://doi.org/10.1038/nri3495.

Barbar, L., Jain, T., Zimmer, M., Kruglikov, I., Sadick, J.S., Wang, M., Kalpana, K., Rose, I.V.L., Burstein, S.R., Rusielewicz, T., Nijsure, M., Guttenplan, K.A., di Domenico, A., Croft, G., Zhang, B., Nobuta, H., Hebert, J.M., Liddelow, S.A., Fossati, V., 2020. CD49f is a novel marker of functional and reactive Human iPSC-Derived astrocytes. Neuron 107 (3). https://doi.org/10.1016/j.neuron.2020.05.014, 436-453 e412.

Belanger, M., Allaman, I., Magistretti, P.J., 2011. Brain energy metabolism: focus on astrocyte-neuron metabolic cooperation. Cell Metab. 14 (6), 724–738. https://doi.org/10.1016/j.cmet.2011.08.016.

Bonnet, E., Touyarot, K., Alfos, S., Pallet, V., Higueret, P., Abrous, D.N., 2008. Retinoic acid restores adult hippocampal neurogenesis and reverses spatial memory deficit in vitamin A deprived rats. PLoS One 3 (10), e3487. https://doi.org/10.1371/journal.pone.0003487.

Cargill, R., Kohama, S.G., Struve, J., Su, W., Banine, F., Witkowski, E., Back, S.A., Sherman, L.S., 2012. Astrocytes in aged nonhuman primate brain gray matter synthesize excess hyaluronan. Neurobiol. Aging 33 (4). https://doi.org/10.1016/j.neurobiolaging.2011.07.006, 830 e813-824.

Chambers, S.M., Fasano, C.A., Papapetrou, E.P., Tomishima, M., Sadelain, M., Studer, L., 2009. Highly efficient neural conversion of human ES and iPS cells by dual inhibition of SMAD signaling. Nat. Biotechnol. 27 (3), 275–280. https://doi.org/10.1038/nbt.1529.

Chatterjee, A., Chatterji, U., 2017. All-trans retinoic acid ameliorates arsenic-induced oxidative stress and apoptosis in the rat uterus by modulating MAPK signaling proteins. J. Cell. Biochem. 118 (11), 3796–3809. https://doi.org/10.1002/jcb.26029.

Chen, Q., Ma, Y., Ross, A.C., 2002. Opposing cytokine-specific effects of all trans-retinoic acid on the activation and expression of signal transducer and activator of transcription (STAT)-1 in THP-1 cells. Immunology 107 (2), 199–208. https://doi.org/10.1046/j.1365-2567.2002.01485.x.

Chen, B.W., Zhang, K.W., Chen, S.J., Yang, C., Li, P.G., 2021. Vitamin A deficiency exacerbates gut microbiota dysbiosis and cognitive deficits in amyloid precursor protein/presenilin 1 transgenic mice. Front. Aging Neurosci. 13, 753351. https://doi.org/10.3389/fnagi.2021.753351.

Chen, Z.P., Wang, S., Zhao, X., Fang, W., Wang, Z., Ye, H., Wang, M.J., Ke, L., Huang, T., Lv, P., Jiang, X., Zhang, Q., Li, L., Xie, S.T., Zhu, J.N., Hang, C., Chen, D., Liu, X., Yan, C., 2023. Lipid-accumulated reactive astrocytes promote disease progression in epilepsy. Nat. Neurosci. 26 (4), 542–554. https://doi.org/10.1038/s41593-023-01288-6.

Chi, H., Barry, S.P., Roth, R.J., Wu, J.J., Jones, E.A., Bennett, A.M., Flavell, R.A., 2006. Dynamic regulation of pro- and anti-inflammatory cytokines by MAPK phosphatase 1 (MKP-1) in innate immune responses. Proc. Natl. Acad. Sci. U. S. A. 103 (7), 2274–2279. https://doi.org/10.1073/pnas.0510965103.

Chung, W.S., Allen, N.J., Eroglu, C., 2015. Astrocytes control synapse formation, function, and elimination. Cold Spring Harbor Perspect. Biol. 7 (9), a020370. https://doi.org/10.1101/cshperspect.a020370.

Davis, R.J., 2000. Signal transduction by the JNK group of MAP kinases. Cell 103 (2), 239–252. https://doi.org/10.1016/s0092-8674(00)00116-1.

Davis, R.L., Sanchez, A.C., Lindley, D.J., Williams, S.C., Syapin, P.J., 2005. Effects of mechanistically distinct NF-kappaB inhibitors on glial inducible nitric-oxide synthase expression. Nitric Oxide 12 (4), 200–209. https://doi.org/10.1016/j.niox.2005.04.005.di.Masi.

di Masi, A., Leboffe, L., De Marinis, E., Pagano, F., Cicconi, L., Rochette-Egly, C., Lo-Coco, F., Ascenzi, P., Nervi, C., 2015. Retinoic acid receptors: from molecular mechanisms to cancer therapy. Mol Aspects Med 41, 1–115. https://doi.org/10.1016/j.mam.2014.12.003.

Ding, Y., Qiao, A., Wang, Z., Goodwin, J.S., Lee, E.S., Block, M.L., Allsbrook, M., McDonald, M.P., Fan, G.H., 2008. Retinoic acid attenuates beta-amyloid deposition and rescues memory deficits in an Alzheimer's disease transgenic mouse model. J. Neurosci. 28 (45), 11622–11634. https://doi.org/10.1523/JNEUROSCI.3153-08.2008.

Duan, S., Anderson, C.M., Stein, B.A., Swanson, R.A., 1999. Glutamate induces rapid upregulation of astrocyte glutamate transport and cell-surface expression of GLAST. J. Neurosci. 19 (23), 10193–10200. https://doi.org/10.1523/JNEUROSCI.19-23-10193.1999.

Escartin, C., Galea, E., Lakatos, A., O'Callaghan, J.P., Petzold, G.C., Serrano-Pozo, A., Steinhauser, C., Volterra, A., Carmignoto, G., Agarwal, A., Allen, N.J., Araque, A., Barbeito, L., Barzilai, A., Bergles, D.E., Bonvento, G., Butt, A.M., Chen, W.T., Cohen-Salmon, M., Verkhratsky, A., 2021. Reactive astrocyte nomenclature, definitions, and future directions. Nat. Neurosci. 24 (3), 312–325. https://doi.org/10.1038/s41593-020-00783-4.

Ghasemi, M., Mayasi, Y., Hannoun, A., Eslami, S.M., Carandang, R., 2018. Nitric oxide and mitochondrial function in neurological diseases. Neuroscience 376, 48–71. https://doi.org/10.1016/j.neuroscience.2018.02.017.

Gudas, L.J., 2022. Retinoid metabolism: new insights. J. Mol. Endocrinol. 69 (4), T37–T49. https://doi.org/10.1530/JME-22-0082.

Guttenplan, K.A., Weigel, M.K., Prakash, P., Wijewardhane, P.R., Hasel, P., Rufen-Blanchette, U., Munch, A.E., Blum, J.A., Fine, J., Neal, M.C., Bruce, K.D., Gitler, A.D., Chopra, G., Liddelow, S.A., Barres, B.A., 2021. Neurotoxic reactive astrocytes induce cell death via saturated lipids. Nature 599 (7883), 102–107. https://doi.org/10.1038/s41586-021-03960-y.

Ho, S.M., Hartley, B.J., Tcw, J., Beaumont, M., Stafford, K., Slesinger, P.A., Brennand, K.J., 2016. Rapid Ngn2-induction of excitatory neurons from hiPSC-derived neural progenitor cells. Methods 101, 113–124. https://doi.org/10.1016/j.ymeth.2015.11.019.

Huang, Y., Minigh, J., Miles, S., Niles, R.M., 2008. Retinoic acid decreases ATF-2 phosphorylation and sensitizes melanoma cells to taxol-mediated growth inhibition. J. Mol. Signal. 3, 3. https://doi.org/10.1186/1750-2187-3-3.

Hyvarinen, T., Hagman, S., Ristola, M., Sukki, L., Veijula, K., Kreutzer, J., Kallio, P., Narkilahti, S., 2019. Co-stimulation with IL-1beta and TNF-alpha induces an inflammatory reactive astrocyte phenotype with neurosupportive characteristics in a human pluripotent stem cell model system. Sci. Rep. 9 (1), 16944. https://doi.org/10.1038/s41598-019-53414-9.

Kamermans, A., Planting, K.E., Jalink, K., van Horssen, J., de Vries, H.E., 2019. Reactive astrocytes in multiple sclerosis impair neuronal outgrowth through TRPM7-mediated chondroitin sulfate proteoglycan production. Glia 67 (1), 68–77. https://doi.org/10.1002/glia.23526.

Kampmann, E., Johann, S., van Neerven, S., Beyer, C., Mey, J., 2008. Anti-inflammatory effect of retinoic acid on prostaglandin synthesis in cultured cortical astrocytes. J. Neurochem. 106 (1), 320–332. https://doi.org/10.1111/j.1471-4159.2008.05395.x.

Katayama, H., Hama, H., Nagasawa, K., Kurokawa, H., Sugiyama, M., Ando, R., Funata, M., Yoshida, N., Homma, M., Nishimura, T., Takahashi, M., Ishida, Y., Hioki, H., Tsujihata, Y., Miyawaki, A., 2020. Visualizing and modulating mitophagy

for therapeutic studies of neurodegeneration. Cell 181 (5), 1176–1187 e1116. https://doi.org/10.1016/j.cell.2020.04.025.
Khakh, B.S., Sofroniew, M.V., 2015. Diversity of astrocyte functions and phenotypes in neural circuits. Nat. Neurosci. 18 (7), 942–952. https://doi.org/10.1038/nn.4043.
Kim, B., Lee, J.H., Yang, M.S., Jou, I., Joe, E.H., 2008. Retinoic acid enhances prostaglandin E2 production through increased expression of cyclooxygenase-2 and microsomal prostaglandin E synthase-1 in rat brain microglia. J. Neurosci. Res. 86 (6), 1353–1360. https://doi.org/10.1002/jnr.21593.
Kruk, P.K., Nader, K., Skupien-Jaroszek, A., Wojtowicz, T., Buszka, A., Olech-Kochanczyk, G., Wilczynski, G.M., Worch, R., Kalita, K., Wlodarczyk, J., Dzwonek, J., 2023. Astrocytic CD44 deficiency reduces the severity of kainate-induced epilepsy. Cells 12 (11). https://doi.org/10.3390/cells12111483.
Leng, K., Rose, I.V.L., Kim, H., Xia, W., Romero-Fernandez, W., Rooney, B., Koontz, M., Li, E., Ao, Y., Wang, S., Krawczyk, M., Tcw, J., Goate, A., Zhang, Y., Ullian, E.M., Sofroniew, M.V., Fancy, S.P.J., Schrag, M.S., Lippmann, E.S., Kampmann, M., 2022. CRISPRi screens in human iPSC-derived astrocytes elucidate regulators of distinct inflammatory reactive states. Nat. Neurosci. 25 (11), 1528–1542. https://doi.org/10.1038/s41593-022-01180-9.
Li, K.Y., Gong, P.F., Li, J.T., Xu, N.J., Qin, S., 2020. Morphological and molecular alterations of reactive astrocytes without proliferation in cerebral cortex of an APP/PS1 transgenic mouse model and Alzheimer's patients. Glia 68 (11), 2361–2376. https://doi.org/10.1002/glia.23845.
Liddelow, S.A., Guttenplan, K.A., Clarke, L.E., Bennett, F.C., Bohlen, C.J., Schirmer, L., Bennett, M.L., Munch, A.E., Chung, W.S., Peterson, T.C., Wilton, D.K., Frouin, A., Napier, B.A., Panicker, N., Kumar, M., Buckwalter, M.S., Rowitch, D.H., Dawson, V. L., Dawson, T.M., Barres, B.A., 2017. Neurotoxic reactive astrocytes are induced by activated microglia. Nature 541 (7638), 481–487. https://doi.org/10.1038/nature21029.
Liu, T., Zhang, L., Joo, D., Sun, S.C., 2017. NF-kappaB signaling in inflammation. Signal Transduct. Targeted Ther. 2, 17023. https://doi.org/10.1038/sigtrans.2017.23.
Maden, M., 2007. Retinoic acid in the development, regeneration and maintenance of the nervous system. Nat. Rev. Neurosci. 8 (10), 755–765. https://doi.org/10.1038/nrn2212.
Manetsch, M., Che, W., Seidel, P., Chen, Y., Ammit, A.J., 2012. MKP-1: a negative feedback effector that represses MAPK-mediated pro-inflammatory signaling pathways and cytokine secretion in human airway smooth muscle cells. Cell. Signal. 24 (4), 907–913. https://doi.org/10.1016/j.cellsig.2011.12.013.
Medzhitov, R., 2008. Origin and physiological roles of inflammation. Nature 454 (7203), 428–435. https://doi.org/10.1038/nature07201.
Mizee, M.R., Nijland, P.G., van der Pol, S.M., Drexhage, J.A., van Het Hof, B., Mebius, R., van der Valk, P., van Horssen, J., Reijerkerk, A., de Vries, H.E., 2014. Astrocyte-derived retinoic acid: a novel regulator of blood-brain barrier function in multiple sclerosis. Acta Neuropathol. 128 (5), 691–703. https://doi.org/10.1007/s00401-014-1335-6.
Napoli, J.L., 2012. Physiological insights into all-trans-retinoic acid biosynthesis. Biochim. Biophys. Acta 1821 (1), 152–167. https://doi.org/10.1016/j.bbalip.2011.05.004.
Napoli, J.L., 2017. Cellular retinoid binding-proteins, CRBP, CRABP, FABP5: effects on retinoid metabolism, function and related diseases. Pharmacol. Ther. 173, 19–33. https://doi.org/10.1016/j.pharmthera.2017.01.004.
Pamies, D., Sartori, C., Schvartz, D., Gonzalez-Ruiz, V., Pellerin, L., Nunes, C., Tavel, D., Maillard, V., Boccard, J., Rudaz, S., Sanchez, J.C., Zurich, M.G., 2021. Neuroinflammatory response to TNFalpha and IL1beta cytokines is accompanied by an increase in glycolysis in human astrocytes in vitro. Int. J. Mol. Sci. 22 (8). https://doi.org/10.3390/ijms22084065.
Pickles, S., Vigie, P., Youle, R.J., 2018. Mitophagy and quality control mechanisms in mitochondrial maintenance. Curr. Biol. 28 (4), R170–R185. https://doi.org/10.1016/j.cub.2018.01.004.
Robb, J.L., Hammad, N.A., Weightman Potter, P.G., Chilton, J.K., Beall, C., Ellacott, K.L. J., 2020. The metabolic response to inflammation in astrocytes is regulated by nuclear factor-kappa B signaling. Glia 68 (11), 2246–2263. https://doi.org/10.1002/glia.23835.
Seo, S., Park, M.J., Park, M.G., Gwak, M., Kim, Y., Jang, J., Hong, N., Lee, B.S., Kim, C., Jo, S., Shim, H.B., Kim, H.J., Kim, M.H., Yoo, S.H., Yoon, S., Kim, S., Lee, J.H., Choi, S.H., Lee, S.Y., Kim, H., 2025. DHRS13 suppresses differentiation and mitophagy in glioma via retinoic acid and mitochondrial reactive oxygen species. Nat. Commun. 16 (1), 6996. https://doi.org/10.1038/s41467-025-62148-4.
Sofroniew, M.V., Vinters, H.V., 2010. Astrocytes: biology and pathology. Acta Neuropathol. 119 (1), 7–35. https://doi.org/10.1007/s00401-009-0619-8.
Stewart, V.C., Heales, S.J., 2003. Nitric oxide-induced mitochondrial dysfunction: implications for neurodegeneration. Free Radic. Biol. Med. 34 (3), 287–303. https://doi.org/10.1016/s0891-5849(02)01327-8.
van Neerven, S., Regen, T., Wolf, D., Nemes, A., Johann, S., Beyer, C., Hanisch, U.K., Mey, J., 2010. Inflammatory chemokine release of astrocytes in vitro is reduced by all-trans retinoic acid. J. Neurochem. 114 (5), 1511–1526. https://doi.org/10.1111/j.1471-4159.2010.06867.x.
Vanden Berghe, W., Plaisance, S., Boone, E., De Bosscher, K., Schmitz, M.L., Fiers, W., Haegeman, G., 1998. p38 and extracellular signal-regulated kinase mitogen-activated protein kinase pathways are required for nuclear factor-kappaB p65 transactivation mediated by tumor necrosis factor. J. Biol. Chem. 273 (6), 3285–3290. https://doi.org/10.1074/jbc.273.6.3285.
Vermeulen, L., De Wilde, G., Van Damme, P., Vanden Berghe, W., Haegeman, G., 2003. Transcriptional activation of the NF-kappaB p65 subunit by mitogen- and stress-activated protein kinase-1 (MSK1). EMBO J. 22 (6), 1313–1324. https://doi.org/10.1093/emboj/cdg139.
Wang, L., Hagemann, T.L., Kalwa, H., Michel, T., Messing, A., Feany, M.B., 2015. Nitric oxide mediates glial-induced neurodegeneration in Alexander disease. Nat. Commun. 6, 8966. https://doi.org/10.1038/ncomms9966.
Xin, M., Jin, H., Guo, X., Zhao, L., Li, X., Xu, D., Zheng, L., Liu, L., 2025. Retinoic acid ameliorates rheumatoid arthritis by attenuating inflammation and modulating macrophage polarization through MKP-1/MAPK signaling pathway. KOREAN J. PHYSIOL. PHARMACOL. 29 (1), 45–56. https://doi.org/10.4196/kjpp.24.079.
Xu, J., Drew, P.D., 2006. 9-Cis-retinoic acid suppresses inflammatory responses of microglia and astrocytes. J. Neuroimmunol. 171 (1-2), 135–144. https://doi.org/10.1016/j.jneuroim.2005.10.004.
Yen, A., Roberson, M.S., Varvayanis, S., Lee, A.T., 1998. Retinoic acid induced mitogen-activated protein (MAP)/extracellular signal-regulated kinase (ERK) kinase-dependent MAP kinase activation needed to elicit HL-60 cell differentiation and growth arrest. Cancer Res. 58 (14), 3163–3172. https://www.ncbi.nlm.nih.gov/pubmed/9679985.
Yeon, G.B., Shin, W.H., Yoo, S.H., Kim, D., Jeon, B.M., Park, W.U., Bae, Y., Park, J.Y., You, S., Na, D., Kim, D.S., 2021. NFIB induces functional astrocytes from human pluripotent stem cell-derived neural precursor cells mimicking in vivo astrogliogenesis. J. Cell. Physiol. 236 (11), 7625–7641. https://doi.org/10.1002/jcp.30405.
Zamanian, J.L., Xu, L., Foo, L.C., Nouri, N., Zhou, L., Giffard, R.G., Barres, B.A., 2012. Genomic analysis of reactive astrogliosis. J. Neurosci. 32 (18), 6391–6410. https://doi.org/10.1523/JNEUROSCI.6221-11.2012.
Zhang, S., Shi, R., Chen, S., Wei, X., Zhou, Q., Wang, Y., 2018. All-trans retinoic acid inhibits the proliferation of SGC7901 cells by regulating caveolin-1 localization via the ERK/MAPK signaling pathway. Oncol. Lett. 15 (2), 1523–1528. https://doi.org/10.3892/ol.2017.7499.
Zhang, L., Xu, Z., Jia, Z., Cai, S., Wu, Q., Liu, X., Hu, X., Bai, T., Chen, Y., Li, T., Liu, Z., Wu, B., Zhu, J., Zhou, H., 2025. Modulating mTOR-dependent astrocyte substate transitions to alleviate neurodegeneration. Nat. Aging 5 (3), 468–485. https://doi.org/10.1038/s43587-024-00792-z.
Zhou, X.F., Shen, X.Q., Shemshedini, L., 1999. Ligand-activated retinoic acid receptor inhibits AP-1 transactivation by disrupting c-Jun/c-Fos dimerization. Mol. Endocrinol. 13 (2), 276–285. https://doi.org/10.1210/mend.13.2.0237.